

Evaluation of inter-site variability of NorSand calibrations and advancing screening level assessment of state parameter for platinum tailings dams in Southern Africa

Gregory Mc Donald, Pieter Francois Oelofse, Nika Mincione, Tinus Grobler
SRK Consulting ZA, Johannesburg, South Africa, gmcDonald@srk.co.za

Bryce Marcotte, Dmitri Bohach
SRK Consulting CA, Saskatoon, Canada

ABSTRACT: The Bushveld Igneous Complex (BIC) and the Great Dyke of Southern Africa are recognized as hosting the largest reserves of platinum group metals (PGMs) globally. Within this region, three PGM-bearing geological units exist in proximity yet exhibit distinctly varying platinum orebody mineralogies. This natural variability leads to observable differences in the index properties and in-situ behaviour of the tailings derived from these units, despite similarities in processing and deposition. As most platinum tailings storage facilities (TSFs) within the BIC and Great Dyke are raised using the upstream method, the density (state) of these tailings is paramount to overall stability. The interpreted state of the tailings often determines whether a facility is “stable” or requires costly remedial measures to meet current standards. This study presents a comparative evaluation of the in-situ state of platinum tailings sourced from four platinum TSFs: each derived from a unique geological unit within the BIC or Great Dyke. The critical state of platinum group metal (PGM) tailings was evaluated using the cavity expansion model (Shuttle & Jefferies 1998; Shuttle & Jefferies 2016), calibrated for representative samples with Norsand constitutive models. Calibrations were validated against published data for recent Platreef tailings studies. Results show that the characteristic in situ state for these platinum tailings do not correlate well with the conventional “Plewes et al.” screening approach, with the latter suggesting more dilative behaviour. These findings highlight the importance of a unique calibration for assessing liquefaction potential and informing effective design of upstream tailings dams.

KEYWORDS: NorSand, widget calibration, platinum tailings, state parameter, liquefaction assessment, tailings storage facilities.

1 INTRODUCTION

The Bushveld Igneous Complex (BIC) in South Africa and the Great Dyke in Zimbabwe are globally renowned for hosting the largest reserves of platinum group metals (PGMs). These regions are critical to the global supply of PGMs, which are essential for various industrial applications, including catalytic converters, electronics, and renewable energy technologies.

Platinum tailings storage facilities (TSFs) in the BIC and Great Dyke are predominantly constructed using the upstream method, where the interpreted in-situ relative density, or state, of the tailings plays a critical role in determining whether a TSF is deemed stable or requires costly remedial measures to meet global safety and operational standards.

This paper presents a comparative evaluation of the in-situ state of platinum tailings sourced from four TSFs, each associated with a unique geological unit within the BIC or Great Dyke.

The NorSand critical state constitutive model was calibrated for representative samples from each site to quantify and compare the state parameters of the tailings. The calibration process followed the Jefferies & Been (2016) CPTu-based methodology based on the work of Shuttle & Jefferies (1998) and was benchmarked against data from other non-plastic materials, including calibration chamber studies and a recent investigation of Platreef tailings (Ayala et al. 2022)..

2 GEOLOGICAL SETTING

Figure 1 shows the locations of the Southern African platinum belts and the locations of the platinum TSFs referred to in this paper. The acronyms of each site indicated on the figure are described in Section 5.

2.1 Bushveld Igneous Complex Deposits (South Africa)

The BIC hosts three principal PGM deposits associated with different mechanisms of PGM mineralisation developed within varying stratigraphic and structural contexts of this layered

mafic intrusion, and which exhibit distinct geological characteristics despite their common origin within the Rustenburg Layered Suite (Cawthorn et al. 2002). The chromite-rich Upper Group 2 (UG2) Reef where platinum occurs between chromite grains requiring specialised processing to separate metals from the hard chromitite host (Mondal & Mathez, 2007); the Merensky Reef, a pyroxenite layer with chromite bands containing PGMs alongside copper, nickel, and gold (Coetzee, 1976); and the Platreef, a contact-type deposit of mixed rock types formed where the intrusion met sedimentary rocks (McDonald et al. 2005).

2.2 Great Dyke Main Sulphide Zone (Zimbabwe)

The Great Dyke represents a fundamentally different geological environment through its Main Sulphide Zone - a 550 km long, narrow intrusion cutting through ancient rocks. The Main Sulphide Zone along the dyke occurs as a 2-4 m thick layer within pyroxenite host rocks, with platinum concentrated in sulphide minerals rather than chromite (Piña et al. 2016).

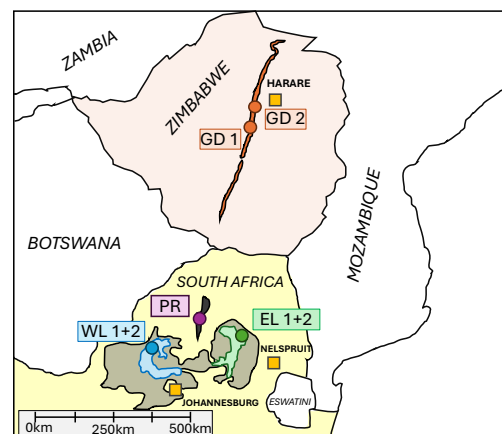


Figure 1. Locality map showing the platinum belts in Southern Africa.

2.3 Geotechnical Challenges

Regardless of the proximity of these reef systems within a relatively confined geological region, and despite employing similar processing methods (milling and flotation), variations in host rock lithology and mineralogy, necessitate different grinding intensities and flotation chemistries, resulting in tailings with measurably different particle and geotechnical characteristics, such as particle morphology, specific gravity (G_s) and Atterberg limits.

3 NORSAND

Developed by Jefferies (1993), NorSand is a critical state-based model that gained widespread adoption following major tailings dam failures, where it was used in failure investigations and risk assessments (Jefferies et al. 2019).

3.1 Model Framework and Capabilities

NorSand is a generalised critical state model based on the state parameter (ψ), which is defined as the difference between the current void ratio and the critical state void ratio at the current mean effective stress (Jefferies & Been, 2015). The framework enables the model to capture the unique material behaviour of non-plastic particulate geomaterials across a wide range of densities and stress conditions, making it particularly suitable for modelling mine tailings.

The model's advantage lies in its ability to simulate both contractive and dilative behaviour, strain-softening responses and, the static liquefaction phenomenon that has been responsible for catastrophic tailings dam failures (Reid et al. 2023). Unlike traditional elastic-plastic constitutive models, NorSand incorporates the state-dependent nature of soil behaviour, where the same material can exhibit significantly different responses depending on its initial density and mean effective stress.

3.2 Application of NorSand in the tailings sphere

NorSand has achieved state-of-the-art status in tailings engineering, as evidenced by its adoption in major failure back analyses, including those of the Mount Polley (2014), Fundão (2015), and Cadia (2018) disasters.

According to Reid et al. (2023), NorSand has established itself as the industry best practice for evaluating static liquefaction potential, with extensive uptake among geotechnical consultancies and regulatory agencies. The constitutive model offers several technical advantages to model strain softening deformation behaviour. Shuttle & Jefferies (2016) highlight the model's ability to capture the full stress-strain response of tailings materials, including post-peak softening behaviour that is critical for understanding progressive failure mechanisms. Furthermore, NorSand can be used to estimate soil behaviour measured with a cone penetration test (CPT) through the CPT Widget (Shuttle, 2019) methodology of cavity expansion modelling. This approach is an efficient workflow for in-situ characterization of tailings deposits (Fourie et al. 2022).

4 NORSAND WIDGET & CPTU STATE PARAMETER INVERSION

CPT penetration within an infinite medium can be idealised through a cavity expansion framework. Carter et al. (1986) demonstrated a numerical solution to a cohesive-frictional material using cavity expansion theory. However, closed formed solutions do not exist for more advanced constitutive models such as Norsand. The CPT Widget employs a finite element model to simulate cavity expansion of the soil (Shuttle

& Jefferies, 2016). Based on the computed numerical response, a relationship between the normalized tip resistance as measured by the cone (Q_p) and the state (ψ) of the soil can be established. This cavity expansion-based approach represents a significant advancement over traditional empirical CPT interpretation methods, as it explicitly accounts for soil-specific behaviour through material-calibrated NorSand parameters rather than relying on correlations.

4.1 CPT inversion parameters

The CPT Widget facilitates the determination of two inversion parameters, denoted as \bar{k} and \bar{m} , which define the mathematical relationship between measured cone penetration resistance and the in-situ state parameter. The hat on the inversion parameter indicates a drained calibration. These inversion parameters are typically estimated empirically based on case histories (Plewes et al. 1992; Jefferies & Been 2016), providing engineers with a screening tool to quantify the in-situ state.

The inversion parameter \bar{k} represents the intercept coefficient in the CPT-state parameter relationship, effectively defining the baseline cone resistance for a given soil at critical state conditions ($\psi = 0$). The parameter \bar{m} controls the slope of this relationship, determining how sensitively the cone resistance responds to changes in soil density relative to the critical state.

To move past a screening assessment, the \bar{k} and \bar{m} inversion parameters are determined through the numerical simulation of cone penetration across a variety of soil states and boundary conditions of the cone. The cavity expansion simulations are performed for combinations of mean effective stress (p'), initial (in-situ) state parameter (ψ_0), and rigidity index (I_r). The simulations are repeated for both drained and undrained boundary conditions, to characterise the full range of expected responses encountered during investigations. The simulated normalized cone tip resistance based on spherical cavity expansion (Q_{widget}) values are plotted against the corresponding soil state.

The unique \bar{k} and \bar{m} values determined for a round of simulations are plotted logarithmically against I_r to account for soil elasticity. This approach ensures that the resulting CPT calibration reflects variations in soil stiffness.

4.2 State parameter from the Widget

Once the inversion parameters \bar{k} and \bar{m} have been calibrated for the specific tailings material, the in-situ state parameter can be directly determined from measured cone penetration data using the relationship Equation (1):

$$\psi = -\frac{1}{\bar{m}} \ln(Q_p / \bar{k}) \quad (1)$$

Where Q_p , in this instance, represents the mean normalised cone tip resistance obtained from field CPT soundings. One important consideration in making use of Equation (1) is the in-situ coefficient of lateral earth pressure, K_0 , which is either estimated through field tests (Oelofse, 2026; Narainsamy, 2025) or assumed. Equation (2) and (3) provide the method to compute the normalised tip resistance from in-situ soundings:

$$Q_p(1 - B_q) + 1 = \bar{k} \exp(-\bar{m} \psi) \quad (2)$$

$$Q_p = 3((q_t - u) / \sigma'_{v0}) / (1 + 2K_0) \quad (3)$$

Where B_q (the normalised excess pore pressure ratio) provides a measure of the drainage condition during penetration, and which was used to determine the appropriate widget calibration (drained or undrained) to be applied to the calculation of state.

4.3 Limitations of the widget method

Despite widespread adoption, the NorSand Widget has notable limitations in tailings applications. The method cannot accurately model partially drained cone penetration conditions commonly encountered in some silty tailings materials, as it assumes either fully drained or undrained penetration (Smith et al. 2021, Ayala et al. 2022).

Additionally, historical calibration chamber (CC) databases were predominantly developed using clean sands (low to zero fines) at dense, dilative states rather than the loose, contractive conditions typical of TSFs (Ayala et al. 2022). Furthermore, calibration chamber case histories specifically for platinum tailings remain limited, with only recent studies (e.g., Ayala et al. 2022) beginning to address this gap, necessitating reliance on triaxial-based calibrations as presented herein.

5 CALIBRATED PLATINUM TAILINGS

To address the lack of platinum tailings case histories and compliment the Ayala (2022) work which, in part, published on upstream platinum tailings, the objective of this paper is to present a set of calibrated NorSand parameters for four platinum TSF sites, each representing different platinum ore bodies as follows:

- WL Western limb, BIC
- EL Eastern limb, BIC (after Bohach et al. 2025)
- GD Great Dyke of Zimbabwe
- PR Platreef, BIC (after Ayala, 2022; Ayala et al. 2022)

The suffix numbers 1 and 2 differentiate between coarse - "1" and fine - "2" fractions of tailings material selected from each respective site. It should be noted that regarding the "PR" calibrations presented, insufficient information was available to determine whether multiple calibrations were conducted, precluding any definitive classification of particle size distribution (PSD) for this dataset.

Some important notes to consider, is that the WL1 material, is of Merensky reef origin only, WL2, EL1 and EL2 include a combination of UG2 reef which contain a chrome content and Merensky reef tailings, GD1 comprised surficial samples from a single site in Zimbabwe and GD2 consisted of piston samples collected at depth from a different site adjacent to the mine in question. This distinction makes GD1 and GD2 slightly different from the WL and EL calibrations sets.

5.1 Material classification

Figure 2 presents the combined PSD envelopes for each platinum site. Representative samples are differentiated by line type, with solid lines indicating coarse fractions and dashed lines representing fine fractions for each respective site.

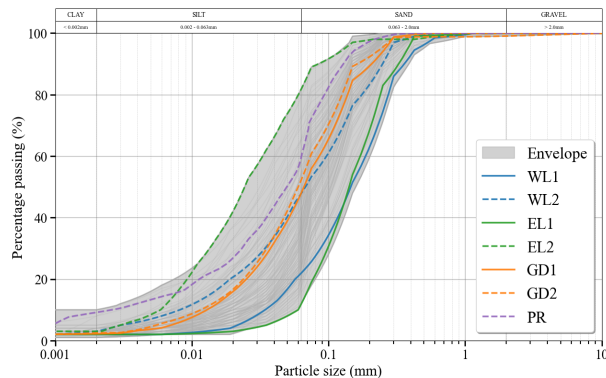


Figure 2. Particle size distribution of selected sites.

Table 1 presents index properties for each calibration, highlighting variations in G_s across the different gradations.

While platinum tailings generally exhibit non-plastic to low-plasticity behaviour, notable variability exists: GD1, GD2, and PR materials show low to moderate plasticity, whereas WL1, WL2, and EL1 show no plasticity, reflecting potential differences in geological origins and processing histories. These variations occur both between sites (inter-site) and within facilities (intra-site) due to evolving deposition conditions, segregation and material source changes. Plasticity Index (PI) and fines content (FC) may serve as practical proxies for identifying when different NorSand calibrations are warranted.

Table 1. Foundation indicators of the platinum sites.

Parameter	WL1	WL2	EL1	EL2	GD1	GD2	PR
G_s	3.21	3.00	3.85	3.38	3.23	3.23	2.97
LL	0	0	0	23.7	25.7	25.5	24.0
PL	0	0	0	11.7	21.9	21.8	18.0
PI	0	0	0	12.0	3.8	3.7	6.0
FC (%)	26	53	19	89	56	61	72
$USCS$	SM	ML	SM	CL	SM-ML	ML	CL

5.2 NorSand calibrations of platinum sites

Triaxial compression testing was conducted on reconstituted samples from each site to establish the constitutive model parameters. A testing program comprising both isotropically consolidated drained (CID) and undrained (CIU) tests was implemented to define the critical state framework for each material. Subsequently under methods described in Jefferies & Been (2016), CID tests on dense specimens exhibiting dilative behaviour were performed to determine the state-dilatancy parameter (χ_{tc}) and volumetric coupling coefficient (N).

For the WL and EL materials, the small-strain shear modulus (G_{max}) degradation curve was established through literature-based correlations combined with forward iterative modelling techniques. Conversely, the Great Dyke (GD 1 & 2) and Platreef (PR) samples were subjected to bender element testing to directly measure the shear wave velocity and derive the corresponding stiffness degradation relationships. Table 2 presents the NorSand calibrations of the various platinum sites. The reference calibrations for EL 1 & 2 (Bohach et al. 2025) and PR (Ayala, 2022) materials were incorporated from previous published studies to contribute towards a comparative framework for this study.

Table 2. NorSand calibration parameters for the platinum sites.

Parameter	WL1	WL2	EL1	EL2	GD1	GD2	PR
λ_{10}	0.08	0.13	0.08	0.12	0.08	0.09	0.09
Γ_{1kPa}	0.83	0.82	0.98	1.07	0.96	0.94	0.83
M_{tc}	1.42	1.45	1.37	1.50	1.45	1.41	1.47
N	0.18	0.3	0.35	0.2	0.4	0.5	0.25
χ_{tc}	3.35	3.2	2.85	2.5	3.0	4.0	2.7
H_0	52	30	54	50	140	135	100
H_ψ	88	50	472	450	1300	1225	1090
G_{ref} (MPa)	35	41	32	32	74	62	30
n	0.6	0.4	0.5	0.5	0.6	0.7	0.7
ν	0.17	0.18	0.2	0.2	0.2	0.2	0.2

Examination of the calibration parameters derived from the platinum tailings datasets reveals several notable trends.

Critical state parameters:

- λ_{10} : Consistently narrow range of 0.07 to 0.13 across all sites.
- Γ : Ranges from 0.82 to 1.07, indicating relatively similar critical state lines.
- M_{tc} : Values of 1.37 to 1.5, suggesting consistent critical state strength characteristics.

Plastic behaviour:

- χ_{ic} : Ranges from 2.5 to 4, indicating comparable dilatancy responses despite different geological origins.
- H_{ψ} : WL1 and WL2 materials exhibit markedly lower values (50-88) compared to other sites (450-1300).
- H_0 : Relatively consistent across all sites.

Elastic stiffness parameters:

- G_{max} and n (elastic stiffness exponent): Definitive conclusions cannot be established, as direct bender element measurements were only conducted on GD and PR materials, limiting comparative analysis.

5.3 Cone penetration comparison

Figure 3 compares the site specific correlations between the critical state line slope (λ_{10}) and the CPT friction sleeve ratio (F_r), to the Plewes et al. (1992) correlation.

Scatter plots are used in Figure 3 to demonstrate the spread of the site-specific data with respect to the Plewes method, per recommendations by Torres-Cruz (2021). Vertical error bars represent the variability in λ_{10} obtained from triaxial testing, while horizontal error bars denote the 10th and 90th percentile range of F_r from CPTu soundings.

The characteristic F_r values for the PR site were not available to supplement this study. Instead, the relationship proposed by Plewes et al. (1992) was applied to provide context for the platinum site's position relative to the other sites.

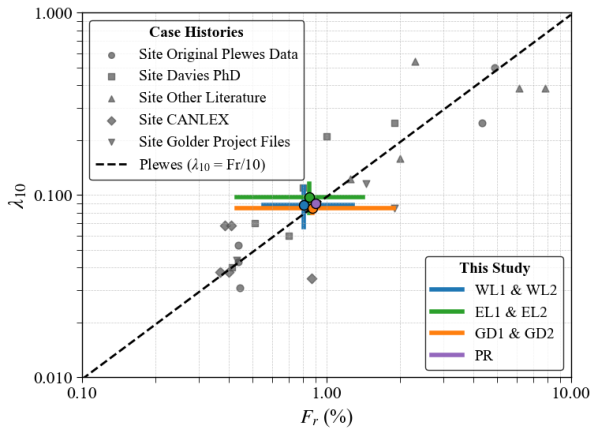


Figure 3. Site specific calibration, CSL slope (λ_{10}) against friction ratio (F_r) compared to (Plewes et al. 1992) (after Bohach et al. 2025).

Particularly noteworthy is the agreement between the mean λ_{10} and F_r values for the platinum sites, represented by circular plot markers, which independently cluster within a consistent range. Figure 3 highlights the uncertainty inherent in the Plewes method and emphasises the need for caution when applying it to assess the liquefaction potential of site-specific tailings, as suggested by Torres-Cruz (2021).

5.4 Inversion parameter comparison

The drained inversion parameters from the finite element modelling of each calibration are presented in Table 3 for each

site. As discussed in Section 4.1, the inversion parameters are a function of I_r , which is typically presented as a function of \bar{k}_1 , \bar{k}_2 and \bar{m}_1 , \bar{m}_2 , as shown by Equation (4) below:

$$\bar{k}, \bar{m} = \bar{k}_1, \bar{m}_1 \ln(I_r) + \bar{k}_2, \bar{m}_2 \quad (4)$$

Where \bar{k}_1, \bar{m}_1 are scaling coefficients and \bar{k}_2, \bar{m}_2 are logarithmic offsets.

For the PR calibration, the widget method was simulated for I_r of 50 – 400 and ψ of -0.05 to 0.11 for $p' = 100$ and 500. The results were fitted to provide a relationship for the inversion parameters \bar{k} and \bar{m} for completeness.

Table 3. Widget inversion parameters of platinum sites.

Parameter	WL1	WL2	EL1	EL2	GD1	GD2	PR*
\bar{k}_1	2.161	1.722	2.164	2.308	5.313	4.641	3.61
\bar{k}_2	19.21	16.64	17.03	16.32	11.67	14.82	14.9
\bar{m}_1	0.480	0.641	0.721	0.721	1.049	1.093	1.37
\bar{m}_2	3.867	2.530	3.678	3.678	3.766	4.904	2.34

PR* - estimated from Ayala (2022) for purpose of presentation.

Plewes et al. (1992) developed the relationship of \bar{k} and \bar{m} with calibration chamber testing on dense sands which showed a relationship of M_{tc} to \bar{k} and λ_{10} to \bar{m} . Plewes et al. (1992) suggested that the inversion parameters of the soil can be estimated with Equation (5) and (6) below:

$$\bar{k} = \left(3 + \frac{0.85}{\lambda_{10}}\right) M_{tc} \quad (5)$$

$$\bar{m} = 11.9 - 13.3\lambda_{10} \quad (6)$$

Where M_{tc} can be measured from laboratory triaxial compression tests, and λ_{10} can be estimated from F_r as given in Figure 3.

Figure 4 shows the inversion parameters, \bar{k} and \bar{m} , which relate the simulated Q_p and ψ to the λ_{10} of the material. A clear observation of this case study is that despite significant variations in geomorphology and rheology across the different sites, the data consistently cluster within a narrow region of one another, outlying the trends suggested by Plewes et al. (1992).

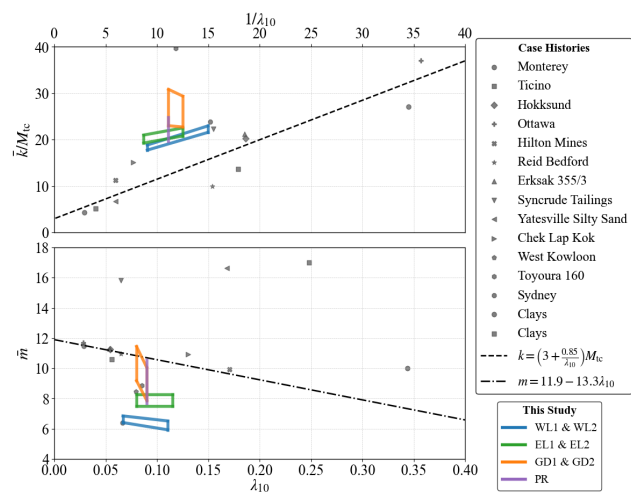


Figure 4. Comparison of inversion Widget parameters to Plewes et al (1992) estimations (after Bohach et al. 2025)

In Figure 5, the simulated tailings Q_p and ψ trends are not consistent with the data used to develop the Plewes et al. (1992)

screening method. The platinum tailings all have a larger \bar{k} and smaller \bar{m} value. This would result in a lower prediction of in-situ state (more dilative) for the Plewes et al. (1992) screening method as compared to the Widget method for all calibrations considered, which, highlights the need to move past screening level interpretations for sensitive projects.

5.5 Characteristic state from the widget

The trends for the platinum sites illustrated in Figure 5 indicate that, despite their diverse geological origins, the sites fall within a relatively narrow parametric space. This suggests similarities in the critical state behaviour of widget simulations. The shaded regions associated with each site designation allude to the potential range of calibration variability for coarse and fine fractions. The unscaled Widget simulation and calibration chamber results are presented for the PR material (Ayala et al. 2022) which agrees well with the other platinum sites.

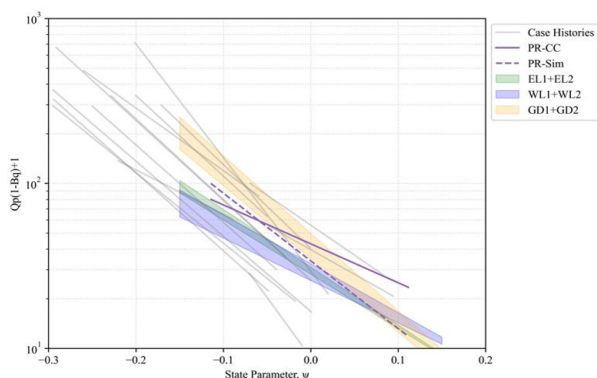


Figure 5. Simulated Q_p and ψ relationships for the platinum sites.

5.6 Implications of risk

Figure 6 illustrates the relative impact of applying the Widget method compared to Plewes et al. (1992) for sites EL1 and GD2. For EL1, the Plewes approach characterises the majority of the profile as dilative ($\psi < -0.05$, green shading), suggesting strain-hardening behaviour and low liquefaction susceptibility. In contrast, the Widget calibration reveals the material to be almost entirely contractive ($\psi > -0.05$, red shading), indicating significant liquefaction potential and lower associated undrained shear strengths. The GD2 profile demonstrates an equally concerning pattern; while Plewes identifies much of the material as moderately contractive, the Widget approach shows substantially more contractive behaviour.

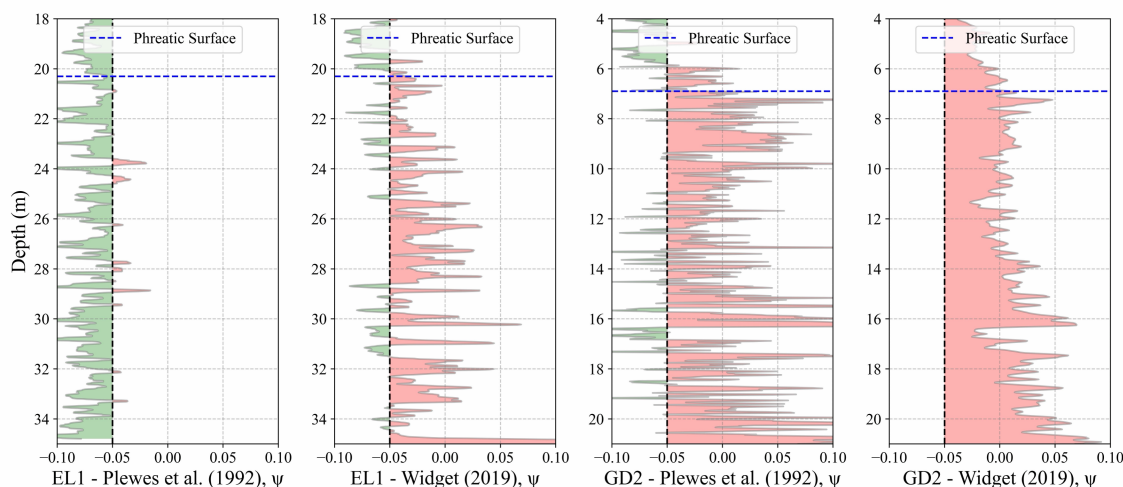


Figure 6. Relative implication of state parameter when applying the Widget method compared to Plewes et al (1992) for EL1 and GD2.

This demonstrates that conventional screening methods can underestimate the degree of contractiveness and therefore the associated liquefaction risk, for these facilities. For tailings facilities where stability is governed by the competence of the deposited tailings, mischaracterisation of material state could lead to unconservative assessments of factor of safety, potentially overlooking the need for remedial measures such as buttressing or retrofitted drainage systems.

6 DISCUSSION

The authors recognise that the standalone NorSand Widget methodology does not represent a definitive solution for platinum tailings characterisation.

Further research is required to address the complex nature of in-situ material behaviour, necessitating comprehensive calibration chamber testing programs tailored to each specific tailings material, noted by Shuttle & Cunning (2007) and Been (2016). While this approach may present practical limitations, a potential solution involves utilising a "MiniCal" approach (Ayala, 2022), which requires substantially reduced material quantities for physical modelling applications.

The reliability of the Widget approach can be substantially improved supported by integrating high-quality intact sampling campaigns, coupled with the appropriate laboratory testing and conducting in-situ stress level calibrations for the site. An added benefit of high-quality sampling during a site characterisation campaign, is that the gravimetric water content and specific gravity can be used to verify the performance of the widget method. This is achieved by computing the in-situ state parameter from the recovered samples (Bohach et al. 2024; Shuttle and Jefferies 2016) or examining the range of void ratios values for the corresponding sounding.

While alternative methods are not expected to match the widget output exactly, owing to sample disturbance, it can still provide a reasonable indication of the overall behaviour. As shown by Oelofse (2024), CPTu-derived samples, such as MOSTAP samples, can provide reliable results in platinum tailings if a methodical approach is applied when extracting, transporting and testing the samples, to determine the in-situ densities and void ratio.

This study has shown that platinum tailings as a broad grouping can have significant differences in PSD, mineralogy, Atterberg limits and, ultimately, NorSand behaviour. It is therefore pertinent to highlight that the adoption of a dataset or calibration from a different site of the same tailings mineral type should be used with caution.

For example, the range of state parameter for a given Q_p of ± 40 , can provide a ψ range of -0.07 to +0.03 – a range of ≈ 0.1 , depending on the chosen calibration for a platinum tailings site. Therefore, a generalisation of parameters by mineral type is not reasonable and site-specific calibrations are a requisite when performing beyond screening level assessments of the facility such as the Shuttle & Jefferies (2016) CPT Widget methodology.

7 CONCLUSIONS

This investigation presents NorSand constitutive model calibrations derived from remoulded triaxial testing programs conducted on materials from four upstream platinum tailings storage facilities. Representative fine and coarse fractions were characterised for each site to capture the range of material properties encountered in these deposits.

The implementation of the NorSand Widget simulation methodology across all sites has established a valuable case history dataset specifically tailored to platinum tailings materials. This dataset addresses a significant gap in the literature.

The study revealed notable differences between the Widget-derived inversion parameters and those estimated using the established Plewes et al. (1992) correlation for parameters \bar{k} and \bar{m} . This illustrates the limitations of applying generalised empirical relationships to platinum tailings materials and emphasises the importance of material-specific calibration approaches. The findings suggest that platinum tailings exhibit unique behavioural characteristics. Further work is required to ensure reliable assessment of in-situ state conditions and liquefaction susceptibility.

This investigation aimed to expand upon existing case histories of platinum tailings deposits and establish a reference framework to motivate future assessments to extend beyond conventional screening-level evaluations for similar facilities.

8 ACKNOWLEDGEMENTS

The Authors gratefully acknowledge SRK Consulting, including SRK Consulting (Canada) Inc. and SRK Consulting (South Africa) ENGEO, for the opportunity to present these case studies. Sincere appreciation is extended to the mining sector and associated mining houses for providing the invaluable field and laboratory datasets that allowed for this comparative study and contribution to platinum tailings case histories and site characterisation methodologies.

9 REFERENCES

Ayala, J., 2022. Assessment of the state parameter in mine tailings using cone penetration tests with calibration chambers. PhD thesis. University of Western Australia.

Ayala, J., Fourie, A. and Reid, D., 2022. Improved cone penetration test predictions of the state parameter of loose mine tailings. *Canadian Geotechnical Journal*, 59(11), pp.1969-1980.

Been, K., 2016. Characterising mine tailings for geotechnical design. *Australian Geomechanics Journal*, 51(4), pp. 59-78.

Bohach, D., Marcotte, B. and Ketilson, E., 2025. Assessment of insitu state from CPT for an upstream tailings facility founded on high plasticity clay. In: *Proceedings of Tailings and Mine Waste 2025*, Banff, Canada.

Carter, J.P., Booker, J.R. and Yeung, S.K., 1986. Cavity expansion in cohesive frictional soils. *Geotechnique*, 36(3), pp.349-358.

Cawthorn, R. G., Lee, C. A., Schouwstra, R. P. and Mellowship, P., 2002. Relationship between PGE and PGM in the Bushveld Complex. *The Canadian Mineralogist*, 40(2), pp. 311-328.

Coetzee, C. B., 1976. Mineral resources of the Republic of South Africa. 5th ed. Pretoria: Government Printer.

Fourie, A., Verdugo, R., Bjelkevik, A., Torres-Cruz, L.A. and Znidarcic, D., 2022. Geotechnics of mine tailings: a 2022 State of the Art. In: *Proceedings of 20th International Conference on Soil Mechanics and Geotechnical Engineering*, Sydney, Australia.

Jefferies, M. G., 1993. Nor-Sand: a simple critical state model for sand. *Geotechnique*, 43(1), pp. 91-103.

Jefferies, M. and Been, K., 2016. Soil liquefaction: A Critical State Approach. CRC press.

Jefferies, M., Morgenstern, N., Van Zyl, D. and Wates, J., 2019. *Report on NTSF Embankment Failure, Cadia Valley Operations, for Ashurst Australia by Independent Technical Review Board*. 17 April 2019. H356804-00000-22A-230-0001.

McDonald, I., Holwell, D. A. and Armitage, P. E. B., 2005. Geochemistry and mineralogy of the Platreef, northern Bushveld Complex. *Mineralium Deposita*, 40(5), pp. 526-549.

Mondal, S. K. and Mathez, E. A., 2007. Origin of the UG2 chromitite layer, Bushveld Complex. *Journal of Petrology*, 48(3), pp. 495-510.

Narainsamy, Y. 2025. Evolution of the in-situ stress state in an upstream constructed tailings dam. Ph.D. thesis, University of Pretoria.

Oelofse, P.F., 2026. Determination of K0 in-situ in sandy-silt tailings using DMT and CPTu. In: *Proceedings of the 21st International Conference on Soil Mechanics and Geotechnical Engineering*, Vienna, Austria.

Oelofse, P.F., 2024. On the Effectiveness of MOSTAP sampling in Tailings. In: *Proceedings of the 7th International Conference on Geotechnical and Geophysical Site Characterization (ISC 7)*, Barcelona, Spain.

Piña, R., Gervilla, F., Barnes, S.J., Oberthür, T. and Lunar, R., 2016. Platinum-group element concentrations in pyrite from the Main Sulfide Zone of the Great Dyke of Zimbabwe. *Mineralium Deposita*, 51(7), pp.853-872.

Plewes, H. D., Davies, M. P. and Jefferies, M. G., 1992. CPT based screening procedure for evaluating liquefaction susceptibility. In: *Proceedings of the 45th Canadian Geotechnical Conference*, Toronto, ON, October 1992. Vol. 4, pp. 1-9.

Reid, D. and Fourie, A., 2023. Development and outcomes of a tailings slope stability comparative design exercise. *Canadian Geotechnical Journal*, 61(8), pp.1683-1704.

Shuttle, D., & Jefferies, M. (1998). Dimensionless and unbiased CPT interpretation in sand. *International Journal for Numerical and Analytical Methods in Geomechanics*, 22(5), 351-391.

Shuttle, D. (2019). CPTwidget: a finite element program for soil-specific calibration of the CPT. *Geotechnical Research*.

Shuttle, D. A. and Cunning, J., 2007. Liquefaction potential of silts from CPTu. *Canadian Geotechnical Journal*, 44, pp. 1-19.

Shuttle, D. and Jefferies, M., 2016. Determining silt state from CPTu. *Geotechnical Research*, 3(3), pp.90-118.

Smith, K., Reid, D. and Fanni, R., 2021. Comparison of CPTu Inversion Parameters Estimated Using the NorSand Widget. In: *Proceedings of The 7th International Conference on Tailings Management (Tailings 2021)*, Santiago, Chile.

Torres-Cruz, L. A., 2021. The Plewes Method: a Word of Caution. *Mining, Metallurgy and Exploration*, 38, pp.1329-1338.